PHILOSOPHICAL MAGAZINE A, 2000, VOL. 80, NO. 6, 1349–1364

An atomistic study of formation and migration of vacancies in (11$\bar{2}$1) twin boundaries in Ti and Zr

J. R. FERNÁNDEZ*†, A. M. MONTI†, R. C. PASIANOT†‡, and V. VITEK§

† Departamento de Materiales, Comisión Nacional de Energía Atómica, Avenida Libertador 8250, 1429 Capital, Argentina
‡ Consejo Nacional de Investigaciones Científicas y Técnicas, Argentina
§ Department of Material Science and Engineering, University of Pennsylvania, Philadelphia, Pennsylvania 19104-6272, USA

[*Received 10 May 1999 and accepted 10 December 1999*]

ABSTRACT

The formation and migration of vacancies in (11$\bar{2}$1) twin boundaries in α-Ti and α-Zr are studied by computer modelling. Three empirical central force potentials constructed within the embedded-atom method are used to represent atomic interactions. Minimum-energy structures for the grain boundary are found first and the vacancy is then introduced by removing an atom and allowing further relaxation of the structure. Formation energies, entropies and relaxation volumes are calculated for different positions of vacancies. In order to analyse the vacancy migration, and thus the boundary self-diffusion, various vacancy jumps have been investigated and the corresponding migration energies and entropies calculated. The most probable paths composed of these simple jumps are then proposed. Both the formation and the migration free energies are significantly lower than in the bulk which demonstrates the role of the grain boundary as a vacancy sink and a fast diffusion channel. These free energies are then employed in evaluation of the diffusion coefficient tensor, the effective activation energies Q_{jj} and the pre-exponential factors D_{0jj}, when the jj component of this tensor is assumed to follow an Arrhenius relationship $D_{jj} = D_{0jj} \exp\left(-Q_{jj}/k_B T\right)$. The boundary diffusion is then contrasted with the bulk diffusion and the calculated diffusion coefficients compared with available experimental data.

§ 1. INTRODUCTION

Grain boundaries are regions in which the atomic structure differs greatly from that of the bulk (Sutton and Balluffi 1995). Consequently, they display very distinct physical properties that significantly affect and even control the physical and mechanical behaviour of materials. An important property of this type is the atomic transport, which may be several orders of magnitude faster along grain boundaries and other interfaces than in the bulk (Balluffi 1982, Peterson 1983, Kaur and Gust 1988, Kaur *et al.* 1995). Such short-circuiting of the diffusion plays a primary role in many metallurgical processes that take place at usual working temperatures. Typical examples are creep, corrosion, solid-state transformations and penetration of impurities.

* Email: julrfern@cnea.gov.ar

Philosophical Magazine A ISSN 0141–8610 print/ISSN 1460-6992 online
http://www.tandf.co.uk/journals

A fundamental description of the diffusion process in grain boundaries requires understanding of their atomic structures and the mechanism of atomic transport in such structures. Since the atomic structure of grain boundaries is crystal like (Balluffi 1986, Finnis and Rühle 1993, Sutton and Balluffi 1995), the self-diffusion in the boundaries is considered to occur via thermally assisted motion of vacancies, similarly to in the bulk (Balluffi 1982, 1984, Biscondi and Pontikis 1985, Kaur and Gust 1988, Kaur *et al.* 1995) although the structure of interfacial vacancies and their properties may differ significantly from those of the bulk vacancies. Since the structure of interfacial vacancies cannot be investigated directly by available experimental techniques, the present understanding of the local structure of interfacial vacancies is mainly based on computer simulations. The majority of such studies were performed for elemental metals and ordered alloys crystallizing in structures with cubic symmetry employing either pair potentials or many-body central force potentials (Faridi and Crocker 1980, Brokman *et al.* 1981, Kwok *et al.* 1984a,b, Vitek *et al.* 1985, Mishin and Yurovitskii 1991, Nomura *et al.* 1991, Nomura and Adams 1992, Liu and Plimpton 1995, Farkas and Ternes 1996, Mishin and Farkas 1997). A notable exception is the study of the structure and migration of vacancies in hcp metals by De Diego and Bacon (1991) using pair potentials to describe atomic interactions.

In fact, the same applies to experimental studies of grain-boundary diffusion. The majority of these studies have been made for metals and alloys with cubic crystal structures (Kaur and Gust 1988, Kaur *et al.* 1995) while investigation of the boundary diffusion in hexagonal metals has been very limited in spite of the large technological importance of metals such as Ti and Zr. Furthermore, available experimental measurements for Hf (Guthoff *et al.* 1993), Ti (Herzig *et al.* 1991) and Zr (Dyment *et al.* 1991) have all been made for polycrystals and thus no correlation with the boundary structure is available.

In this paper we present an atomistic study of the structure, formation and migration of vacancies in a symmetric tilt boundary corresponding to a twin on the $(11\bar{2}1)$ plane in Ti and Zr. The interaction between the atoms is described by many-body central force potentials of the type known as the embedded atom method (EAM) (Daw and Baskes 1984, Finnis and Sinclair 1984, Daw *et al.* 1993, Foiles 1996). In both these metals a widespread mechanism of the plastic deformation is twinning on $(11\bar{2}1)$ planes (Yoo 1981; Hirth and Lothe 1982) and thus $(11\bar{2}1)$ twins are common interfaces found in these materials.

First, we outline the crystallography of the boundary studied, border conditions and starting configurations employed in atomistic simulations, as well as the three different many-body potentials used to describe atomic interactions. The results of the simulations are initially the grain-boundary structures. The vacancy is then introduced into various positions in the minimum-energy structure and its formation energy, relaxation volume and vibrational formation entropy calculated. Ultimately, the vacancy migration is studied. Both migration energies and entropies are calculated and the most probable paths composed of these simple jumps are then proposed. On the basis of this analysis the tensor of the diffusion coefficient is evaluated. Assuming that the jj component of this tensor follows an Arrhenius relationship, that is $D_{jj} = D_{0jj} \exp\left(-Q_{jj}/k_{\mathrm{B}}T\right)$, the effective activation energies Q_{jj} and pre-exponential factors D_{0jj} are also determined. The boundary diffusion is then contrasted with the bulk diffusion by estimating the ratio of the bulk and boundary diffusion coefficients. Finally, the results of this study are compared with available experimental data.

§ 2. Crystallography of the boundary studied and method of calculation

The boundary studied is characterized by the twinning plane $\mathbf{K}_1 = (11\bar{2}1)$, twinning direction $[\bar{1}\bar{1}26]$, conjugate plane $\mathbf{K}_2 = (0001)$ and conjugate direction $[11\bar{2}0]$ (figure 1) (Christian 1975). Following Serra and Bacon (1986) we have used two basic starting configuration that differ by symmetry. They are shown in the $[1\bar{1}00]$ projections in figures 1 (*a*) and (*b*) respectively. In these figures the circles represent atoms and different symbols denote the different positions of atoms along the $[1\bar{1}00]$ direction. In particular, white triangles, pluses, squares and crosses represent, in this sequence, the four successive layers along this direction in the ideal hcp lattice. The white triangles and white squares correspond to atoms belonging to the (0001) plane

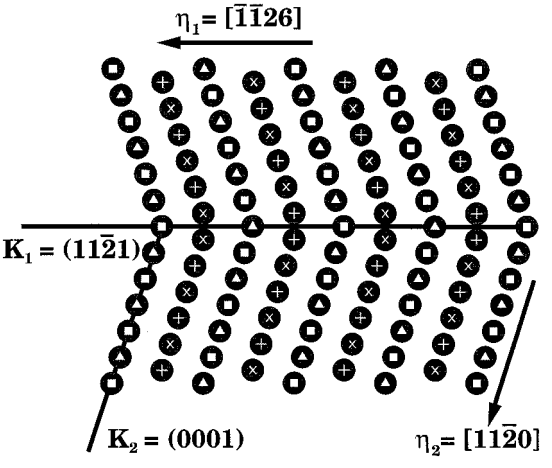

(*a*)

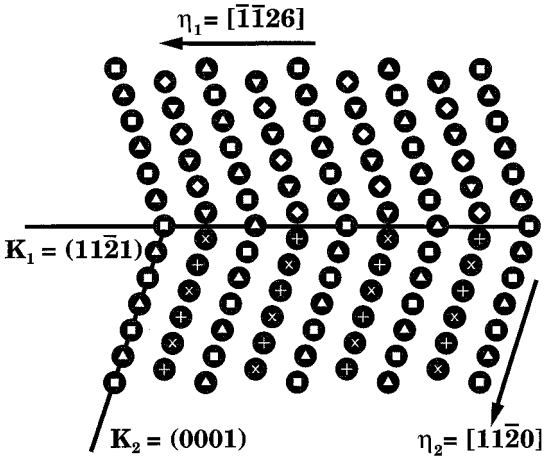

(*b*)

Figure 1. The $[1\bar{1}00]$ projections of the two structures of the $(11\bar{2}1)$ twin boundaries used as starting configurations in atomistic simulations: (*a*) structure R; (*b*) structure D.

in the position A of the ABAB stacking formed by these planes; the white pluses and white crosses correspond to atoms that belong to the (0001) plane in the position B. In the structure shown in figure 1 (*a*), denoted in the following as R; the stacking ABAB is the same in both grains and the structure possesses a mirror symmetry with respect to the reflection in the interfacial plane. In the structure shown in figure 1 (*b*), denoted in the following as D, the stacking in the lower grain is ABAB but in the upper grain ACAC. The atoms that belong to the plane C are represented by inverted white triangles and white diamonds respectively; the four successive layers along the $[1\bar{1}00]$ direction in the upper grain are then depicted by white triangles, inverted triangles, squares and diamonds. This structure is invariant with respect to the 180° rotation around the axis parallel to the $[\bar{1}\bar{1}26]$ direction.

In order to determine the structure of the $(11\bar{2}1)$ twin boundary a bicrystal with this boundary, having the corresponding R or D symmetry, was initially constructed geometrically as described above. Molecular statics employing a gradient method was then used to relax the structure so as to minimize the energy with respect to positions of individual atoms and relative rigid-body displacements of the adjoining grains both parallel and perpendicular to the boundary plane. As a result, no average stresses either tangential or normal to the interface are present in the relaxed structure. (For more details see, for example, Sutton (1984) and Vitek (1996)). During the relaxation periodic boundary conditions have been applied in two directions parallel to the boundary plane ($[\bar{1}\bar{1}26]$ and $[1\bar{1}00]$). Normal to the boundary plane, the upper and the lower grains have been taken as semi-infinite slabs although in practice the atoms remained in perfect lattice positions beyond the tenth layer away from the boundary on either side. The relaxation was regarded as complete when the force acting on any of the atoms did not exceed 10^{-3} eV Å^{-1}.

The formation and migration of vacancies were then studied for the lowest-energy structure found in the structural calculations. These simulations were performed using a spherical cluster, composed of about 4000 atoms, centred at the vacancy, with the boundary passing through this cluster; this geometry is best suited to this purpose owing to the almost spherical symmetry of the point defect studied. While the structural studies were constant-pressure calculations, allowing for the expansion and contraction of the block, the calculations involving vacancies have been made at constant volume so that no expansion and contraction of the spherical cluster were allowed. More details of these calculations are presented together with the results.

A necessary precursor of any atomistic calculation is an appropriate description of atomic interactions. In the present study the energy of the system was described by many-body central-force potentials of EAM type that have been constructed for Ti and Zr in the past. In particular, we used two different potentials for Ti, the first constructed by Fernández *et al.* (1996) and the second by Ackland (1992), and a potential for Zr constructed by Pasianot and Monti (1999). In the following the two potentials for Ti are denoted Ti1 and Ti2 respectively. All these potentials are fitted so as to reproduce the lattice parameters a and c of the corresponding hexagonal lattice, cohesive energy, elastic moduli and, approximately, the vacancy formation energy. A limitation of these potentials is that they do not include any possible effect of covalent bonding that may play a role in transition metals due to unfilled d shell (Pettifor 1995, Pettifor *et al.* 1995). This could be alleviated by using methods that include the covalent-type d bond, such as the recently constructed bond-order potentials for Ti (Girshick *et al.* 1998). However, the calculations employing this method

are more than an order of magnitude time consuming than those using EAM type potentials. At the same time, a recent analysis (Paidar *et al.* 1999) demonstrated that the non-central character of atomic interactions is not very significant when considering structures in which separations of the first-nearest neighbours are significantly different when compared with the perfect lattice. This is the case for grain boundaries and vacancies and thus the EAM-type potentials can be expected to be an adequate approximation for these studies.

§ 3. Structure of the boundary

Several distinct relaxed boundary configurations were found for each potential used. They are characterized by different relative displacements of the grains and different energies and are generally different for different potentials. This is a common phenomenon met in previous atomistic studies of grain boundaries, called structural multiplicity (Wang *et al.* 1984, Vitek *et al.* 1985). However, the lowest-energy structure has been found to be very similar for all the potentials used. Its energy is in all cases four to five times lower than those of the alternate structures. For example, in the case of the Ti2 potential its energy is $150\,\mathrm{mJ\,m^{-2}}$, while the next lowest energy is $622\,\mathrm{mJ\,m^{-2}}$; for Zr the corresponding energies are 102 and $501\,\mathrm{mJ\,m^{-2}}$ respectively. The structure of the boundary with the lowest energy is shown in figure 2. In all cases studied this structure was obtained when using the D structure as a starting configuration. The relaxed structure preserves the symmetry of this configuration, that is invariance with respect to the rotation around the axis parallel to the $[\bar{1}\bar{1}26]$ direction lying in the boundary plane. However, comparison of figure 2 with figure 1 (*b*) reveals that in the relaxed structure the stacking of the (0001) planes is ABAB in both the lower and the upper grains, unlike in the starting configuration in which the stacking in the upper grain is ACAC. Thus the result of the relaxation is the displacement of A layers in the upper grain into the B positions and C layers into A positions without changing the overall symmetry of the structure.

A similar low-energy structure was found by other researchers using different potentials (Serra and Bacon 1986, Farkas 1994). Hence, while the multiple higher-energy structures vary with the potentials used, the low-energy structure appears to be very insensitive to the details of the description of atomic interactions. This implies that the low-energy structure is likely to display properties common to different hcp metals and the following study of vacancies has been made for this structure.

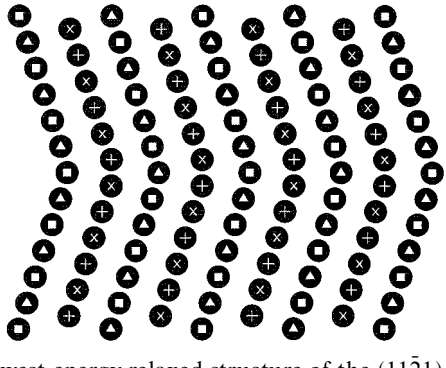

Figure 2. The lowest-energy relaxed structure of the $(11\bar{2}1)$ twin boundary.

§ 4. Structure, formation and migration of grain-boundary vacancies

A vacancy has always been introduced by removing one atom from the relaxed grain boundary and allowing the local atomic neighbourhood to relax again. As explained in § 2, a spherical simulation cell centred at the vacancy was used in these calculations and rigid boundary (constant volume) conditions imposed. Since the two atomic sites at a given $(11\bar{2}1)$ plane are equivalent in the D structure, only one vacancy per layer needs to be investigated. In all cases studied, the vacancy was found to be well localized and fully identified with the initial atomic location. This was the case even for vacancies positioned very near the central layer, where the inward relaxation of the first neighbours is about ten times more than in the bulk.

The formation energy of a vacancy created by the removal of an atom is, by definition,

$$E^{\mathrm{f}} = U_{N-1} - U_N - E_{\mathrm{c}}, \tag{1}$$

where U_N is the energy of the relaxed block (with the grain boundary) containing N atoms before the vacancy has been formed, U_{N-1} the energy of the relaxed block containing $N-1$ atoms after the vacancy has been formed and E_{c} the cohesive energy. The relaxation volume $\Delta\Omega$ associated with the vacancy is determined, to the first order, via the dipole tensor $\mathbf{P}$ as (Schober and Ingle 1980, Schober and Petry 1993)

$$\Delta\Omega = \frac{\mathrm{Tr}\,(\mathbf{P})}{3B}, \tag{2}$$

where B is the bulk modulus. The dipole tensor is related to the stress induced by the defect in the constant volume calculations and equals minus the moment of the forces that have to be applied to the atoms in the rigid border region in order to maintain them in fixed positions. Its components are defined as

$$P_{\gamma\delta} = -\sum_{\ell} F_{\gamma}^{\ell} R_{\delta}^{\ell}, \tag{3}$$

where F_{γ}^{ℓ} is the γ component of the force acting on the atom ℓ and R_{δ}^{ℓ} is the δ component of the position vector of this atom; the summation extends over all the atoms in the rigid border region.

The dependence of the vacancy formation energy on the distance from the boundary plane is shown in figure 3 where it is plotted as a function of the layer index n for all three potentials used; $n = 0$ corresponds to the boundary plane. It is seen that E^{f} has a constant bulk value for $n \geqslant 5$ and it decreases significantly towards the boundary plane. The variation in the relaxation volume, normalized by the atomic volume Ω_0, with the distance from the boundary plane is shown in figure 4. It can be seen that its absolute value increases rapidly when $n \to 0$.

Finally, the vibrational entropy of vacancy formation, calculated in the approximation of independent oscillators, is given as (Hatcher *et al.* 1979)

$$S^{\mathrm{f}} = k_{\mathrm{B}} \ln \left(\prod_{i=1}^{3N} \omega_i^0 \Big/ \prod_{i=1}^{3N} \omega_i \right), \tag{4}$$

where ω_i^0 are the atomic frequencies in the block with the grain boundary before the vacancy was formed and ω_i the corresponding frequencies after the vacancy was formed; k_{B} is the Boltzmann constant. The products extend over all the atoms in

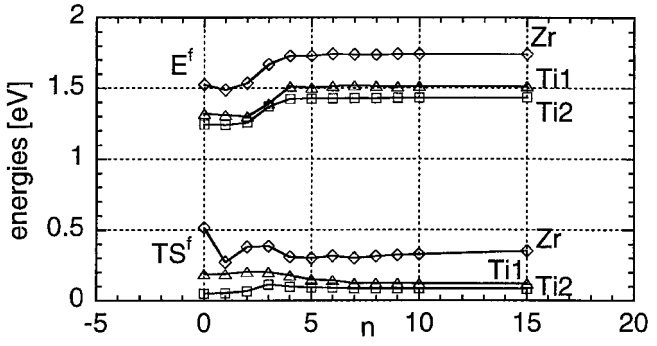

Figure 3. Vacancy formation energy and entropy contributions to the free energy of vacancy formation at the temperature of 1000 K as a function of the distance from the boundary, denoted by the layer index n.

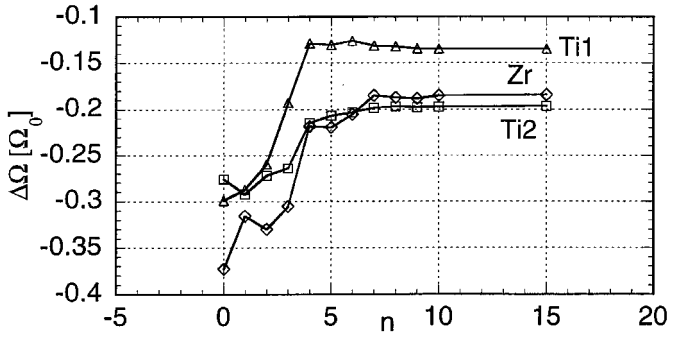

Figure 4. Vacancy relaxation volume (in units of the atomic volume) as a function of the distance from the boundary, denoted by the layer index n.

the relaxed spherical cell as well as in the rigid border region. In this study, S^{f} was first calculated at constant volume and then corrected for constant pressure using the well known thermodynamic relationship (Flynn 1972) $S^{\mathrm{f}}|_p = S^{\mathrm{f}}|_V + B\alpha\,\Delta\Omega$ where B is the bulk modulus and the volumetric thermal expansion coefficient consistent with the potentials used ($3.4 \times 10^{-5}\,\mathrm{K}^{-1}$ for Ti1, $3.6 \times 10^{-5}\,\mathrm{K}^{-1}$ for Ti2 and $-0.34 \times 10^{-5}\,\mathrm{K}^{-1}$ for Zr) (Fernández *et al.* 2000). The value of TS^{f} as a function of n is shown in the lower part of figure 3 for $T = 1000\,\mathrm{K}$, which is a temperature for which significant grain boundary diffusion can be expected. It is seen that this contribution to the free energy of the vacancy formation may be up to one third of E^{f} at the boundary. Furthermore, the dependence of S^{f} on n is more sensitive to the potential used than the corresponding dependencies of E^{f} and $\Delta\Omega$.

In the perfect hcp lattice there are only two distinct atomic jumps between the first-neighbour positions. However, in the vicinity of a grain boundary, many different short jumps can occur owing to the loss of translational symmetry in the direction perpendicular to the boundary plane. In order to facilitate the study of these jumps we assembled a list of neighbours of each atom between layers -5 and $+5$ in the repeat cell of the D grain-boundary structure. The neighbours are defined somewhat arbitrarily such that the maximum length of the jump is $1.35a$, where a is the basal lattice parameter. The total number of possible jumps that is covered by

this list is about 270. However, owing to the symmetry of the grain-boundary structure some of these jumps are equivalent and, when considering only the non-equivalent jumps, the number of jumps that have to be analysed is reduced to about 40.

The energy barriers for the migrational paths of the vacancies have been evaluated as follows. First, a reaction coordinate is chosen that connects the initial and final positions of the moving atom. The moving atom is then placed to various locations along this line, while all the other atoms are at each step relaxed so as to minimize the total energy. The maximum energy found during the passage of the moving atom from the initial to the final position is then identified with the migration energy E^{m}. Figure 5 is a $[1\bar{1}00]$ projection of the grain boundary structure showing the numbering used to describe the jumps. This numbering is the same as that employed by De Diego and Bacon (1991). The numbers stand for the layer index n and the letters indicate various basal planes. The period in the $[\bar{1}\bar{1}26]$ direction is $\{\mathrm{aba'b'}\}$ and planes such as a and a′ are crystallographically equivalent (see figure 1); sites labelled for example, a and $\underline{\mathrm{a}}$ are of the same type but are displaced with respect to each other by one period along the direction of the tilt axis, $[1\bar{1}00]$. The migration energies associated with various jumps are summarized in table 1; the corresponding migration energies in the bulk are shown in table 2. It is seen that some migration energies, for example 2a → 0a, may be one order of magnitude lower than in the bulk.

The vibrational vacancy migration entropy can be calculated similarly to the formation entropy in the approximation of independent oscillators (Vineyard 1957). It is

$$S^{\mathrm{m}} = k_{\mathrm{B}} \ln \left(\prod_{i=1}^{3N-1} \omega_i \Big/ \prod_{i=1}^{3N-1} \omega_i' \right), \tag{5}$$

where ω_i and ω_i' are the ith vibrational mode of the system with the moving atom in the initial configuration and the saddle-point configuration respectively; the former corresponds to the configuration after the vacancy has been formed. In the saddle-point configuration there are only $3N-1$ real frequencies since in the direction of the motion the eigenmode is unstable. In this formulation the vibrational frequency corresponding to the eigenmode that brings the system into the saddle-point configuration (the attempt frequency) was also removed and it is taken into account separately when evaluating frequencies of vacancy jumps. Table 3 presents the vacancy migration entropy calculated using equation (5) for the jumps with the lowest migration energy. The corresponding migration energies in the bulk are shown in table 4.

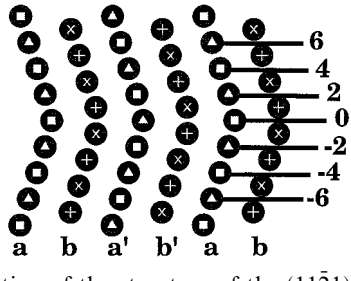

Figure 5. The $[1\bar{1}00]$ projection of the structure of the $(11\bar{2}1)$ twin boundary showing the numbering used to describe the diffusional jumps.

Table 1. Vacancy migration energies evaluated for various jumps using the three different potentials. Jumps are labelled according to the indexing system of figure 5. Sites a and a are positioned in two different neighbouring boundary periods along the tilt axis.

		Energy (eV)					Energy (eV)					Energy (eV)		
from	to	Ti1	Ti2	Zr	from	to	Ti1	Ti2	Zr	from	to	Ti1	Ti2	Zr
0a	1b	0.277	0.549	0.283	1b	0a	0.279	0.557	0.348	2a	0a	0.056	0.398	0.220
	1b′	0.435	0.645	0.438		0a′	0.437	0.653	0.503		0a	0.707	1.168	0.852
	2a	0.130	0.425	0.261		−1b	0.044	0.355	0.150		1b	0.499	0.679	0.410
	2a	0.780	1.195	0.893		−1b	0.763	1.240	0.927		1b′	0.148	0.456	0.226
	3b	0.827	1.056	0.951		2a	0.423	0.714	0.516		−1b	1.635	1.955	1.656
	3b′	2.327	2.646	2.381		2a′	0.224	0.491	0.332		−1b′	1.122	1.453	1.166
	4a	0.553	0.739	0.615		−2a	1.711	1.990	1.762		−2a	0.267	0.437	0.310
						−2a′	1.198	1.488	1.271		3b	0.269	0.548	0.376
						3b	0.368	0.680	0.546		3b′	0.511	0.817	0.656
						3b	0.803	1.149	0.944		4a	0.533	0.818	0.790
						−3b	0.449	0.609	0.547		4a	0.699	1.031	0.790
						4a′	0.605	0.840	0.701		5b	0.476	0.752	0.549
						5b	0.532	0.665	0.560		6a	0.506	0.672	0.545

§ 5. Migration paths and diffusion coefficients

In the following we assume that the self-diffusion along grain boundaries takes place by migration of vacancies via the jumps described in the previous section. After a jump α has taken place, either the vacancy may return to the original position by the reversal of this jump or a different jump occurs. The lower the probability of the reverse jump, the higher is the probability that a new jump occurs, that is the lower is the correlation of such jumps (Mishin 1995; Mishin and Herzig 1995). In this way the diffusing atom can cover a long distance through vacancy jumps. Owing to the

Table 2. Bulk migration energies.

	Energy (eV)		
Bulk	Ti1	Ti2	Zr
Basal	0.506	0.727	0.57
Non-basal	0.483	0.782	0.59

Table 3. Vacancy migration entropies for several low-migration-energy jumps. The indexing system is the same as in table 1.

		Entropy (k_B)					Entropy (k_B)					Entropy (k_B)		
from	to	Ti1	Ti2	Zr	from	to	Ti1	Ti2	Zr	from	to	Ti1	Ti2	Zr
0a	1b	0.24	1.36	0.45	1b	0a	0.08	1.34	3.38	2a	0a	1.01	1.16	4.89
	2a	0.09	1.40	3.37		−1b	0.73	1.28	2.13		1b′	1.52	0.95	1.77
						2a′	−0.41	1.03	2.83		−2a	2.18	0.40	0.37

Table 4. Bulk migration entropies.

	Entropy (k_B)		
Bulk	Ti1	Ti2	Zr
Basal	3.68	1.59	5.93
Non-basal	2.19	2.40	6.36

periodicity of the grain boundary the random walk of a vacancy can be thought of as composed of various simple paths between equivalent positions. Each path will occur with a frequency depending on the migration energies and entropies involved in individual jumps and the number of paths that contribute significantly will be increasing with increasing temperature.

Grain-boundary diffusion is best quantified by the grain-boundary diffusion coefficient which is generally a tensor. For example, the xx component of this tensor is (Ma and Balluffi 1994)

$$D_{xx} = \frac{1}{2}\sum_{\alpha=1}^{N} \nu_\alpha x_\alpha^2 n_\alpha f_{x\alpha} \exp\left(\frac{S_\alpha}{k_B}\right) \exp\left(-\frac{Q_\alpha}{k_B T}\right), \tag{6}$$

where N is the number of non-equivalent jumps α from a lattice site h, ν_α^0 is the attempt frequency of the jump α evaluated in the approximation of independent oscillators, x_α is the x component of the jump, n_α is the fraction of the lattice sites from which a jump α can take place, $f_{x\alpha}$ is the correlation factor in the x direction, $S_\alpha = S_h^f + S_\alpha^m$ is the total entropy and $Q_\alpha = E_h^f + E_\alpha^m$ is the activation energy associated with the jump α; E_h^f and S_h^f are the vacancy formation energy and entropy respectively at the site h. Obviously, the higher the activation energy Q_α, the less the corresponding jump contributes to the diffusion coefficient. Table 5 shows the activation energies of various vacancy jumps in increasing order for each potential used. The horizontal empty line indicates the first ten jumps with the lowest Q_α that are considered when identifying different paths of vacancy migration; for these paths Q_α does not exceed 90% of the bulk activation energy.

The diffusion coefficient, given by equation (6), can be evaluated using a kinetic Monte Carlo technique where diffusion is treated as a correlated walk in a periodic system with multiple jump frequencies. In this case all possible paths are considered and the correlation factors $f_{x\alpha}$ are determined within this scheme (Mishin 1995, Mishin and Herzig 1995). However, we have adopted a simplified approach in which we select several most probable paths for which we can assume that at relevant temperatures the correlation factors are very similar, of the order of one, for all the jumps involved; this is corroborated in the following. In order to analyse the different paths we evaluate the normalized probabilities of vacancy jumps from a given position to a neighbouring site. For a jump α the probability is

$$P_\alpha = \Gamma_\alpha \Big/ \sum_\beta \Gamma_\beta, \tag{7}$$

where $\Gamma_\alpha = \nu_\alpha^0 \exp\left(-G_\alpha^m/k_B T\right)$ is the frequency of the jump α, ν_α^0 is the attempt frequency and $G_\alpha^m = E_\alpha^m - TS_\alpha^m$ is the migration free energy associated with this jump; the summation over β includes all neighbouring sites into which jumps can

Table 5. Activation energies Q_α evaluated for various jumps using the three different potentials. The indexing system is the same as in table 1. Bulk activation energies are also reported.

Jump	Energy, Ti1 (eV)	Jump	Energy, Ti2 (eV)	Jump	Energy, Zr (eV)
(1b; −1b)	1.299	(1b; −1b)	1.531	(1b; −1b)	1.551
(0a; 2a)	1.386	(0a; 2a)	1.609	(0a; 2a)	1.727
(1b; 2a′)	1.478	(2a; −2a)	1.643	(1b; 2a′)	1.733
(0a; 1b)	1.533	(1b; 2a′)	1.668	(0a; 1b)	1.749
(2a; 3b)	1.599	(0a; 1b)	1.733	(2a; −2a)	1.817
(2a; −2a)	1.600	(2a; 3b)	1.759	(2a; 3b)	1.882
(1b; 3b)	1.622	(1b; −3b)	1.789	(0a; 1b′)	1.903
(0a; 1b′)	1.692	(0a; 1b′)	1.829	(1b; 3b)	1.947
(1b; −3b)	1.704	(1b; 5b)	1.841	(1b; −3b)	1.948
(1b; 2a)	1.753	(1b; 3b)	1.857	(1b; 5b)	1.961
(1b; 5b)	1.787	(2a; 6a)	1.883	(2a; 6a)	2.051
(2a; 5b)	1.806	(0a; 4a)	1.923	(2a; 5b)	2.056
(0a; 4a)	1.809	(2a; 5b)	1.963	(0a; 4a)	2.080
Bulk	2.01		2.18		2.33

take place. As the temperature increases the normalized probabilities P_α for a given vacancy jump change in such a way that some of the previously less probable jumps become feasible.

The procedure to find the most probable path for a vacancy is now as follows. We start with the vacancy in a chosen position and let the vacancy jump according to the highest normalized probability that is not a back jump. Once the jump has occurred, we proceed similarly, but now from the new vacancy position. The jumps are then continued until a position equivalent to the starting position is reached. For example, for the Ti1 potential at 300 K, the vacancy starting at 0a position has a probability close to unity of jumping into any of the two symmetric positions 2a or −2a; for the reverse jump the probability is 0.98. From 2a the next most probable jump is to 1b′ with the jump probability 0.02. Once the vacancy jumps into the layer 1 or −1, it is essentially trapped in the jumps (1b; −1b) which do not contribute to the diffusion. The normalized probability of this symmetric jump is almost equal to one and, therefore, highly correlated. The next most probable jump is back to 2a which again does not contribute to the diffusion process. The subsequent possible jump is to 0a′ with the jump probability less than 10^{-4}, which is a position equivalent 0a. The whole sequence of diffusional jumps is then (0a; 2a), (2a; 1b′), (1b′; 0a′). The same is also found for the Ti2 and Zr potentials. This path is indicated in figure 6 as (①). Two other possible paths can occur in which the vacancy crosses the grain boundary plane. They are (0a; 2a), (2a; 1b′), (1b′; −1b′), (−1b′; −2a), (−2a; 0a) (② in figure 6) and (0a; 2a), (2a; −2a), (−2a; 0a) (the same total length as (②) but not shown in figure 6). The former path is found for all three potentials while the latter only for the Ti2 and Zr potentials.

At high temperatures, the number of alternative jumps that a vacancy can accomplish increases. As a result, new and more complicated paths between equivalent positions than those shown in figure 6 may be considered. The overall effect is spreading of the zone in which the vacancy moves, decreasing thus the trapping

power of the grain boundary. For example, the jump (1b; −1b) is no longer as correlated as at low temperatures and alternative jumps, such as (1b; 2a) or (1b; ±3b), may take place. This multiplicity of paths, together with the decrease of the jump correlation, increase the mobility of the vacancy and thus the diffusivity.

In order to compare with the previous case corresponding to 300 K, we consider again the Ti1 potential but now at 1000 K. The vacancy in 0a has lowered the probability of jumping to 2a or −2a positions to 0.78, the reverse jump probability being 0.31. From 2a it has almost the same probability of jumping into −2a, that is crossing the grain boundary centre plane, or to 3b with probabilities 0.21 and 0.22 respectively. From 3b the most probable jumps are to 1b, −1b and the reverse jump to 2a with the jump probabilities 0.56, 0.22 and 0.16 respectively. From (1b) the jumps with the highest probabilities are to −1b (0.48), 3b (0.22), 2a′ (0.13) and −3b (0.08). The most probable paths are thus $\{(0a;2a), (2a;-2a), (-2a;0\underline{a})\}$; $\{(1b;-1b), (-1b;3b), (3b;1\underline{b})\}$; $\{(1b;2a'), (2a';3b'), (3b';1b')\}$ and $\{(1b;2a'), (2a';3b'), (3b';-1b'), (-1b';1b')\}$.

The grain-boundary diffusion coefficient can now be evaluated by inserting into equation (6) the calculated formation and migration energies and entropies together with the attempt frequencies for the vacancy sites and jumps involved in the chosen most probable diffusional paths. These quantities are summarized in table 5; jump entropies not reported in table 3 have been approximated by bulk values. The components of the diffusion coefficient tensor are usually assumed to be well approximated by an Arrhenius-type relation

$$D_{jj} = D_{0jj} \exp\left(-\frac{Q_{jj}}{k_B T}\right), \tag{8}$$

where Q_{jj} is the effective activation energy and D_{0jj} the corresponding pre-exponential factor; jj stands for xx or yy. As an example, figure 7 shows the plot of $\log D_{xx}$ versus $1/k_B T$ for the case of the potential Ti1, which demonstrates the Arrhenius-type behaviour of the diffusion coefficient. In general, using plots of $\log D_{jj}$ versus $1/k_B T$ values of Q_{jj} can be determined from their slopes and the values of D_{0jj} can be found from the same plots by extrapolating to $1/k_B T \to 0$.

Table 6 summarizes the values of Q_{jj} and D_{0jj} determined in this way from the diffusion tensor originally calculated using equation (6). It can be noted that the apparent activation energies for diffusion along the $x \equiv [1\bar{1}00]$ direction are lower

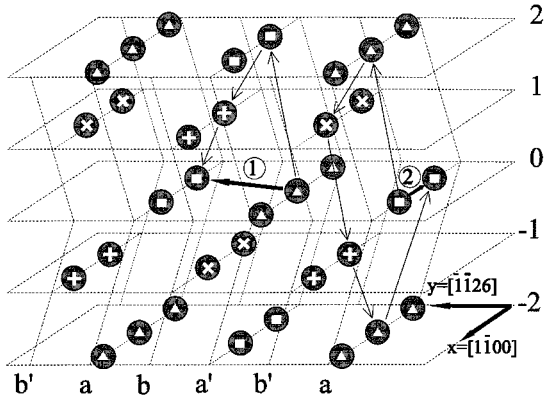

Figure 6. Two possible vacancy paths in the grain boundary studied.

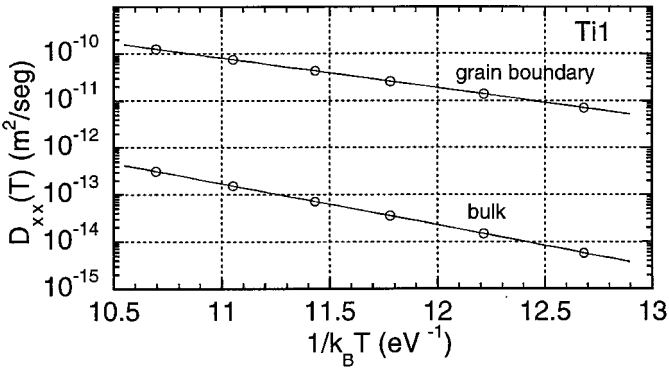

Figure 7. The dependence of the logarithm of the diffusion coefficient calculated using equation (6) on $1/k_BT$. In the case of the grain boundary the D_{xx} component of the diffusion coefficient tensor is shown while for the bulk the basal component is displayed. The reason for this choice is that these diffusion coefficients describe, in both cases, diffusion in the $[1\bar{1}00]$ direction.

Table 6. Effective activation energies Q_{ij} and pre-exponential factors entering equation (8); $x \equiv [1\bar{1}00]$ direction and $y \equiv [11\bar{2}6]$ direction.

	Ti1	Ti2	Zr
D_{0xx} (m^2 s^{-1})	7×10^{-4}	1×10^{-4}	2×10^{-1}
Q_{xx} (eV)	1.45	1.61	1.74
D_{0yy} (m^2 s^{-1})	4×10^{-4}	3×10^{-4}	1×10^{-1}
Q_{yy} (eV)	1.54	1.75	1.81

than those for the $y \equiv [\bar{1}\bar{1}26]$ direction, which suggests a faster diffusion along the tilt axis.

§6. Discussion

In agreement with previous atomistic studies (Serra and Bacon 1986; Farkas 1994), we found that the minimum-energy configuration of the $(11\bar{2}1)$ tilt grain boundary corresponds to the same structure with the D-type symmetry irrespective of the interatomic potential used. This structure, shown in figure 2, has therefore been used in the atomistic studies of vacancies and grain-boundary self-diffusion.

The properties of vacancies formed in the boundary region are significantly different from those of vacancies in the bulk. The formation energy E^f is up to 15% lower and the relaxation volume $\Delta\Omega$ between 50 and 100% larger. These findings are insensitive to the potentials used and agree with those of previous calculations that employed pair potentials (De Diego and Bacon 1991). On the other hand, the formation entropies S^f are sensitive to details of the potentials. However, their contribution to formation free energies is less important than that of E^f; it represents at most one third for $T = 1000$ K, a common temperature at which experimental measurements of grain-boundary diffusion have been made. A similar sensitivity to the potential used is also found in the case of migration entro-

pies, but the obtained range from $0.1k_B$ to $4k_B$ is well within acceptable values (Seeger and Mehrer 1970).

The loss of translational symmetry in the direction perpendicular to the boundary plane results in a great diversity of possible vacancy jumps. It is seen that migration free energies are lower for jumps towards the boundary than for the reverse jumps; this, together with the lower formation free energy, demonstrates that the boundary acts as a sink for vacancies. Also, migration free energies in the grain-boundary region are lower than in the bulk, which results in faster vacancy diffusion. The width of the region in which the formation and migration energies are significantly different from those in the bulk is not more than two or three lattice spacings (approximately 10 Å). This is in good agreement with the usually accepted values of the grain boundary width (for example Herzig *et al.* (1991)).

In several atomistic studies of grain-boundary diffusion (Nomura and Adams 1992, 1995, Ma *et al.* 1993), the formation and migration entropies have been estimated using Zener's (1951) relationship

$$S_h^f = \frac{\beta_z \lambda E_h^f}{T_m}, \qquad S_\alpha^m = \frac{\beta_z \lambda E_\alpha^m}{T_m}, \tag{9}$$

which is based on linear elasticity. Here $\beta_Z = -\mathrm{d}(\mu/\mu_0)/\mathrm{d}(T/T_m)$, where μ is the appropriate elastic modulus at the temperature T and μ_0 the same modulus at 0 K, λ is a constant and T_m the melting temperature; β_Z is assumed to be independent of temperature. Equation (9) implies that S_h^f/E_h^f and S_α^m/E_α^m are equal to the same material-dependent constant. Fernández and Monti (1993) found that this relationship is reasonably well satisfied in the bulk when the lattice relaxation is small. However, equation (9) cannot be expected to hold in high-angle grain boundaries, where local lattice distortions are large. Indeed, the results of the present calculations give $S^f/E^f = 1.7k_B\,\mathrm{eV}^{-1}$ (Ti1), $0.5k_B\,\mathrm{eV}^{-1}$(Ti2), and $3.9k_B\,\mathrm{eV}^{-1}$ (Zr) for the vacancy in the layer $n = 0$. For the fastest jump (1b; −1b) we obtain $S^m/E^m = 16.5k_B\,\mathrm{eV}^{-1}$ (Ti1), $3.6k_B\,\mathrm{eV}^{-1}$ (Ti2) $14.2k_B\,\mathrm{eV}^{-1}$ (Zr) and for the jump (2a; −2a) $8.2k_B\,\mathrm{eV}^{-1}$ (Ti1), $0.9k_B\,\mathrm{eV}^{-1}$ (Ti2) and $1.2k_B\,\mathrm{eV}^{-1}$ (Zr). Hence, Zener's relationship for estimation of the formation and migration entropies is unreliable for grain boundaries.

The activation energies Q_{gb} for grain-boundary self-diffusion are usually in the range 0.5–0.75 of the bulk activation energies Q_b (Kaur and Gust 1988, Kaur *et al.* 1995). Since Q_b measured for ultrapure Ti and Zr are 3.14 eV (Koppers *et al.* 1997) and 3.17 eV (Hood *et al.* 1997) respectively, this implies that $Q_{gb} \approx 1.5$–2.4 eV. This estimation agrees with measurements in grain boundaries for nominally pure α-Ti (Herzig *et al.* 1991). The calculated values of Q_{gb}, shown in table 6, are within this range. However, it should be noted that the calculated ratio Q_{gb}/Q_b is between 0.7 and 0.8. This relatively high ratio of activation energies implies that the calculated grain-boundary diffusion coefficient is only about three orders of magnitude higher than the bulk diffusion coefficient (see figure 7) while experiments suggest a difference of six orders (Vieregge and Herzig 1990, Herzig *et al.* 1991). The reason why the calculated ratio Q_{gd}/Q_b is relatively high is mainly the small difference between the vacancy formation energies in the grain boundary and the bulk (Fernández *et al.* 1996, Pasianot and Monti 1999). This is, presumably, a consequence of a rather special character of the $(11\bar{2}1)$ twin boundaries in which the local environment of boundary atoms is closer to the bulk than in more general boundaries. The experiments were, of course, made for more general boundaries.

The calculated pre-exponential factors D_{0jj} are three orders of magnitude higher for Zr than for Ti, using both the potential Ti1 and the potential Ti2. This difference arises owing to a high-entropy contribution to both the vacancy formation and the vacancy migration in Zr. Indeed, experimental measurements do suggest a higher pre-exponential factor in Zr than in Ti although by only one order of magnitude (Vieregge and Herzig 1990, Herzig *et al.* 1991). This disparity is most probably again related to the rather special character of the boundary studied when compared with general boundaries studied experimentally.

Notwithstanding, the calculations presented in this paper capture all the essential features of grain-boundary diffusion in both Ti and Zr. First, they demonstrate that, in spite of the fact that diffusional processes in the boundary region are very complex, the corresponding components of the tensor of the diffusion coefficient can be characterized by effective activation energies and pre-exponential factors entering an Arrhenius-type relation. Secondly, the diffusion coefficient is at least three orders of magnitude higher in the boundary than in the bulk and it is significantly anisotropic. The width of the boundary region is two or three lattice spacings, as usually assumed. Finally, the calculations not only show that grain-boundary diffusion is faster in Zr than in Ti, as observed, but also demonstrate that in Zr the pre-exponential factor (equation (8)), controlled by the corresponding entropies, is larger than in Ti while the formation and migration energies of vacancies in these two materials do not differ significantly.

Acknowledgements

This research was supported by Consejo Nacional de Investigaciones Científicas y Técnicas (PIP 4205 and PIP 1295) (Argentina) and the National Science Foundation (USA) grant INT93-01102.

References

Ackland, G. J., 1992, *Phil. Mag.* A, **66**, 917.

Balluffi, R. W., 1982, *Metall. Trans.* A, **13**, 2069; 1984, *Diffusion in Crystalline Solids,* edited by G. E. Murch and A. S. Nowick (Orlando, Florida: Academic Press), p. 319; 1986, *Trans. Japan Inst. Metals,* **27**, 23.

Biscondi, M., and Pontikis, V., 1985, *Proceedings of the Fourth Japan Institute of Metals International Symposium on Phenomena,* edited by Y. Ishida *et al.* (Tokyo: Japan Institute of Metals), p. 63.

Brokman, A., Bristowe, P. D., and Balluffi, R. W., 1981, *J. appl. Phys.,* **52**, 6116.

Christian, J. W., 1975, *The Theory of Transformations in Metals and Alloys* (Oxford: Pergamon).

Daw, M. S., and Baskes, M. I., 1984, *Phys. Rev.* B, **29**, 6443.

Daw, M. S., Foiles, S. M., and Baskes, M. I., 1993, *Mater. Sci. Rep.,* **9**, 251.

De Diego, N., and Bacon, D. J., 1991, *Phil. Mag.* A, **63**, 873.

Dyment, F., Iribarren, M. J., Vieregge, K., and Herzig, C., 1991, *Phil. Mag.* A, **63**, 959.

Faridi, B. A., and Crocker, A. G., 1980, *Phil. Mag.* A, **41**, 137.

Farkas, D., 1994, *Metall. Mater. Trans.* A, **25**, 1337.

Farkas, D., and Ternes, K., 1996, *Intermetallics,* **4**, 171.

Fernández, J. R., and Monti, A. M., 1993, *Phys. Stat. sol.* (b), **179**, 337.

Fernández, J. R., Monti, A. M., and Pasianot, R. C., 1996, *J. nucl. Mater.,* **229**, 1; 2000 (to be published).

Finnis, M. W., and Rühle, M., 1993, *Mater. Sci. Technol.,* **1**, 533.

Finnis, M. W., and Sinclair, J. E., 1984, *Phil. Mag.* A, **50**, 45.

Flynn, P., 1972, *Point Defects and Diffusion* (Oxford: Clarendon).

Foiles, S. M., 1996, *Mater. Res. Soc.,* **21**, 24.

GIRSHICK, A., BRATKOVSKY, A. M., PETTIFOR, D. G., and VITEK, V., 1998, *Phil. Mag.* A, **77**, 981.
GUTHOFF, F., MISHIN, Y., and HERZIG, C., 1993, *Z. Metallk.,* **84**, 584.
HATCHER, R. D., ZELLER, R., and DEDERICHS, P. H., 1979, *Phys. Rev.* B, **19**, 5083.
HERZIG, C., WILLECKE, R., and VIEREGGE, K., 1991, *Phil. Mag.* A, **63**, 949.
HIRTH, J. P., and LOTHE, J., 1982, *Theory of Dislocations* (New York: Wiley–Interscience).
HOOD, G. M., ZOU, H., SCHULTZ, R. J., MATSUURA, R. J., ROY, J. A., and JACKMAN, J. A., 1997, *Defect Diffusion Forum,* **143—147**, 49.
KAUR, I., and GUST, W., 1988, *Fundamentals of Grain and Interface Boundary Diffusion* (Stuttgart: Ziegler).
KAUR, I., MISHIN, Y., and GUST, W., 1995, *Fundamentals of Grain and Interface Boundary Diffusion* (Chichester, West Sussex: Wiley).
KOPPERS, M., HERZIG, C., FRIESEL, M., and MISHIN, Y., 1997, *Acta metall. mater.,* **45**, 4181.
KWOK, T., HO, P. S., and YIP, S., 1984a, *Phys. Rev.* B, **29**, 5354; 1984b, *ibid*, **29**, 5363.
LIU, C. L., and PLIMPTON, S. J., 1995, *Phys. Rev.* B, **51**, 4523.
MA, Q., and BALLUFFI, R. W., 1994, *Acta metall. mater.,* **42**, 1.
MA, Q., LIU, C. L., ADAMS, J. B., and BALLUFFI, R. W., 1993, *Acta metall. mater.,* **41**, 143.
MISHIN, Y. M., 1995, *Phil. Mag.* A, **72**, 1589.
MISHIN, Y. M., and FARKAS, D., 1997, *Phil. Mag.* A, **75**, 169.
MISHIN, Y. M., and HERZIG, C., 1995, *Phil. Mag.* A, **71**, 641.
MISHIN, Y. M., and YUROVITSKII, I. V., 1991, *Phil. Mag.* A, **64**, 1239.
NOMURA, M., and ADAMS, J. B., 1992, *J. Mater. Res.,* **7**, 3202; 1995, *ibid.,* **10**, 2916.
NOMURA, M., LEE, S. Y., and ADAMS, J. B., 1991, *J. Mater. Res.,* **6**, 1.
PAIDAR, V., WANG, L. G., SOB, M., and VITEK, V., 1999, *Comput. Simulation Mater. Sci. Engng,* **7**, 369.
PASIANOT, R. C., and MONTI, A. M., 1999, *J. nucl. mater.,* **264**, 198.
PETERSON, N. L., 1983, *Int. Metall. Rev.,* **28**, 65.
PETTIFOR, D. G., 1995, *Bonding and Structure of Molecules and Solids* (Oxford University Press).
PETTIFOR, D. G., AOKI, M., GUMBSCH, P., HORSFIELD, A. P., MANH, D. N., and VITEK, V., 1995, *Mater. Sci. Engng.,* **A192–A193**, 24.
SCHOBER, H. R., and INGLE, K. W., 1980, *J. Phys.* F, **10**, 575.
SCHOBER, H. R., and PETRY, W., 1993, *Mater. Sci. Technol.,* **1**, 289.
SEEGER, A., and MEHRER, H., 1970, *Vacancies and Interstitials in Metals,* edited by A. Seeger, D. Schumacher, W. Schilling and J. Diehl (Amsterdam: North-Holland), p. 1.
SERRA, A., and BACON, D., 1986, *Phil. Mag.* A, **54**, 793.
SUTTON, A. P., 1984, *Int. Metall. Rev.,* **29**, 377.
SUTTON, A. P., and BALLUFFI, R. W., 1995, *Interfaces in Crystalline Materials* (Oxford University Press).
VIEREGGE, K., and HERZIG, C., 1990, *J. nucl. Mater.,* **173**, 118.
VINEYARD, G. H., 1957, *J. Phys. Chem. Solids,* **3**, 121.
VITEK, V., 1996, *Stability of Materials,* NATO Advanced Study Institute Series, edited by A. Gonis, P. E. A. Turchi and J. Kudrnovsky (New York: Plenum), p. 53.
VITEK, V., MINONISHI, Y., and WANG, G. J., 1985, *J. Phys., Paris,* **46**, C4.
WANG, G. J., SUTTON, A. P., and VITEK, V., 1984, *Acta metall.,* **32**, 1093.
YOO, M. H., 1981, *Metall. Trans.* A, **12**, 49.
ZENER, C., 1951, *J. appl. Phys.,* **22**, 372.